The dependence on optical energy of terahertz emission from air plasma induced by two-color femtosecond laser-pulses*

Wu Si-Qing(吴四清)[a)b)], Liu Jin-Song(刘劲松)[a)†], Wang Sheng-Lie(汪盛烈)[a)], and Hu Bing(胡 兵)[a)]

[a)] *Wuhan National Laboratory for Optoelectronics, School of Optical and Electronic Information, Huazhong University of Science and Technology, Wuhan* 430074, *China*

[b)] *School of Electronic and Information Engineering, Hubei University of Science & Technology, Xianning* 437100, *China*

(Received 27 March 2013; revised manuscript received 8 April 2013)

The generation of terahertz (THz) emission from air plasma induced by two-color femtosecond laser pulses is studied on the basis of a transient photocurrent model. While the gas is ionized by the two-color femtosecond laser-pulses composed of the fundamental and its second harmonic, a non-vanishing directional photoelectron current emerges, radiating a THz electromagnetic pulse. The gas ionization processes at three different laser-pulse energies are simulated, and the corresponding THz waveforms and spectra are plotted. The results demonstrate that, by keeping the laser-pulse width and the relative phase between two pulses invariant when the laser energy is at a moderate value, the emitted THz fields are significantly enhanced with a near-linear dependence on the optical energy.

Keywords: terahertz emission, air plasma, femtosecond laser-pulses

PACS: 42.62.Fi, 42.65.Re, 52.38.Dx, 52.25.Jm **DOI:** 10.1088/1674-1056/22/10/104207

1. Introduction

Over the past two decades, the generation of terahertz (THz) waves utilizing air as an emitting medium has incited a great amount of attention due to the potential applications for standoff distance THz wave detection and imaging.[1–4] This method enables the THz wave to be produced near the target, instead of delivering the THz wave from a remote source. So, the intense water vapor absorption of THz waves in the ambient atmosphere can be precluded by transmitting the laser beam. On the other hand, a gas medium has no phonon resonance or echoes owing to THz waves or optical reflection, as often arise in solid state materials commonly employed in THz time domain spectroscopy systems[5–7] such as photon-conductive antennas and electro–optical crystals.[8,9] In addition, from the viewpoint of use-cost, using air as a medium to obtain THz waves is an ideal choice as compared with using the solid materials mentioned above, since there is little or no concern about medium damage.

The earliest report of irradiating a strong laser beam (peak power of 10^{12} W) into air to acquire a THz wave in the atmosphere is from the early 1990s.[1,2] Recently, by utilizing the mixing of a laser's fundamental (ω) waves and its second harmonic (2ω) waves to generate intense THz pulses in air has attracted extensive interest, owing to the remarkable bandwidth and intensity it provides.[3,10,11] For the generation of broadband and strong THz pulses from two-color laser-induced gas plasma, the underlying physical mechanism is initially treated as a four-wave mixing ($\omega+\omega-2\omega$) process.[3,12] However, the third-order nonlinearity is too small to explain some of the subsequently measured results, e.g., the observed THz field strength and saturation[4,13] of THz output, since it originates from bound electrons of ions and free electrons due to ponderomotive or thermal effects.[14] So, Kim *et al.* introduced a so-called transient photocurrent (PC) model, which indicated plasma playing a key role for THz wave generation.[15,16] In this model, excited by a strong laser field, the gas molecules are ionized into plasma, then the freed electrons form a directional transverse current. With the current varying, an electromagnetic pulse at THz spectral range can be generated. However, the method has a drawback: THz field amplitude is proportional to the laser amplitude only when the laser amplitude at a moderate level, which significantly limits the THz field's magnitude. In order to solve this obstacle, Wang *et al.*[17–19] introduced a scheme that uses chirped laser pulses instead of two-color lasers, allowing the generated strong THz amplitudes to scale linearly with the laser amplitude, and achieving a THz field up to tens of MV/cm. Moreover an analytical model is developed to interpret the mechanism of the THz emission.

With respect to the generation of THz pulses from air plasma excited by two-color femtosecond laser pulses, some theoretical and experimental researches have been implemented,[10,20,21] whereas the dependence of the THz emission on the laser-pulses energy is not deeply studied. Here, we focus on this problem mainly in theories and simulations.

*Project supported by the National Natural Science Foundation of China (Grant No. 61177095), the Natural Science Foundation of Hubei Province, China (Grant No. 2012FFA074), the Ph. D. Programs Foundation of Ministry of Education of China (Grant No. 20100142110042), and the Fundamental Research Funds for the Central Universities (Grant Nos. 2012QN094 and 2012QN097).

†Corresponding author. E-mail: jsliu4508@vip.sina.com

© 2013 Chinese Physical Society and IOP Publishing Ltd

2. Theoretical framework

In the radiation of a strong optical field such as high-power femtosecond laser pulses, the air is stimulated and ionized into gas plasma through releasing bound electrons. Under the influence of intense laser pulses, the gas molecules' photoionization has several different hierarchies with the optical intensity varying.[13] At lower laser intensity ($I \leqslant 10^{14}$ W/cm^2, $E \leqslant 10^{10}$ V/m), multiphoton-ionization (MPI) and above-threshold-ionization (ATI) are dominant. At higher laser intensity, tunneling ionization (TI) and over-the-barrier ionization arise, where the laser fields lead to great distortion of the electronic binding potential. In this computation, the laser intensity is estimated to be more than 10^{14} W/cm^2. Hence, TI is the appropriate scheme for the given case.

In the tunneling ionization, two different models for the ionization rate are commonly employed: static tunneling (ST)[22–24] and the Ammosov–Delone–Krainov (ADK) model.[25–27] The two models of the ionization rate possess a similar functional dependence on the electric field but the ST rate is slightly larger than the ADK one at the same laser fields. Here, an ST model is used in the simulations, and the ionization rate $w(t)$ can be described as[28]

$$w(t) = 4w_0 \frac{E_a}{E(t)} \left(\frac{E_\mathrm{i}}{E_\mathrm{h}}\right)^{5/2} \exp\left[-\frac{2}{3}\frac{E_a}{E(t)}\left(\frac{E_\mathrm{i}}{E_\mathrm{h}}\right)^{3/2}\right], \quad (1)$$

where $w_0 = \kappa^2 m e^4/\hbar^3 \approx 4.13 \times 10^{16}$ s^{-1} is the atomic frequency unit ($\kappa = 1/(4\pi\varepsilon_0)$, m and e are the electron mass and charge respectively), $E_\mathrm{h} \approx 13.6$ eV is the ionization potential of hydrogen, $E_\mathrm{i} \approx 15.6$ eV is the ionization potential of the gas molecules in question, approximating air consisting of N_2 entirely. $E_\mathrm{a} = \kappa^3 m^2 e^5/\hbar^4 \approx 5.14 \times 10^{11}$ V/m is the atomic unit of electric field, and $E(t)$ is the amplitude of the employed laser field.

Given the nominal ionization rate $w(t)$, the generated plasma density $\rho(t)$ can be obtained by solving the rate equation[13]

$$\frac{\partial \rho(t)}{\partial t} = w(t)(\rho_0 - \rho(t)), \quad (2)$$

where ρ_0 is the molecular gas initial density. Equation (2) has the solution

$$\rho(t) = \left[\rho(t_0) + \rho_0 \int_{t_0}^{t} w(t') \exp\left(\int_{t_0}^{t'} w(t'')\,\mathrm{d}t''\right)\mathrm{d}t'\right] \times \exp\left(-\int_{t_0}^{t} w(t')\,\mathrm{d}t'\right). \quad (3)$$

Once ionized, the freed electrons will undergo a force from the optical field and disseminate as classical particles. The electron velocity at a subsequent time t is achieved by

$$v(t) = -(e/m)\int_{t_0}^{t} E(t')\,\mathrm{d}t', \quad (4)$$

where t_0 is the instant when the electron is liberated and $E(t)$ is the real electric field. For the initially ionized plasma of atmospheric gas density, the electron–ion collision rate is about 10^{12} s^{-1} under the given conditions, which corresponds to a time between collisions of about 1 ps, much longer than the pulse length of 50 fs used in the simulations. Hence, collision processes during the laser pulse are not taken into account. Note that, in the tunneling ionization model, the ionized electrons are presumed to be motionless at the ionization moment t_0, $v(t_0) = 0$. Then the motive electrons leading to transverse electron current can be taken as[15]

$$J(t) = \int_{t_0}^{t} e v(t,t')\rho_\mathrm{e}(t')\,\mathrm{d}t', \quad (5)$$

where e is the electron charge, t_0 is the initial instant of the ionization process, $v(t,t')$ is the velocity at a time t of electrons born at t', $\rho_\mathrm{e}(t') = w(t')(\rho_0 - \rho(t'))$ denotes the varying rate of the plasma density at t', and $ev(t,t')\rho_\mathrm{e}(t')\,\mathrm{d}t'$ represents the contribution of the ionized electrons at time $t' \sim (t' + \mathrm{d}t')$ to the electron current at a subsequent time t.

In this transient photocurrent model, the time evolving electron current of $J(t)$ can give rise to electromagnetic pulse at THz frequency in the far field, and the strength of the THz field is proportional to the derivative of current density as follows:

$$E_\mathrm{T} \propto \frac{\mathrm{d}J(t)}{\mathrm{d}t}. \quad (6)$$

According to the relation of laser intensity (I) and laser field (E). $I = (\sqrt{\varepsilon/\mu})E^2/2$, and the relation of laser intensity and laser energy (W). $I = (2/\pi)^{3/2}(\phi^2 T_0)^{-1}W$, where ϕ is the optical beam radius and T_0 is the pulse duration (relative to the full width at half maximum (FWHM) width via $T_0 = T_\mathrm{FWHM}/\sqrt{2\ln 2}$),[13] one can easily acquire the expression about the dependence of laser field (E) on laser energy (W), as

$$E = \frac{1}{\phi}\left(\frac{2}{\pi}\right)^{3/4}\sqrt{\frac{2W}{\varepsilon c T_0}}, \quad (7)$$

here, c is the optical velocity ($c = \sqrt{1/(\varepsilon\mu)}$).

On the basis of the above analysis and calculation, we can clearly understand that THz emission (E_T) from air plasma induced by two-color femtosecond laser-pulses depends on laser energy (W), with a complicated functional relationship.

3. Simulations and results discussion

In the simulations, the employed Gaussian laser pulses mixing the fundamental and its second harmonic can be expressed as

$$E(t) = \frac{1}{2}E_{10}\exp(-t^2/T_{10})\,\mathrm{e}^{\mathrm{i}\omega t} + \frac{1}{2}E_{20}\exp(-t^2/T_{20})\,\mathrm{e}^{\mathrm{i}(2\omega t+\theta)}, \quad (8)$$

where ω and 2ω are the fundamental and the second harmonic frequencies, E_{10} and E_{20} are the maximum amplitudes of that two laser fields, T_{10} and T_{20} are their pulse width respectively, and θ is the relative phase between two optical pulses.

Here, the two laser beams utilized are set to the fundamental frequency $\omega(\lambda_1 = 800$ nm) and the second harmonic wave $2\omega(\lambda_2 = 400$ nm). We assume two laser pulses with the same pulse duration of $T_{10,20} = 50$ fs (full width at half maximum (FWHM)), and the relative phase between the fundamental wave and the second harmonic wave is selected to be $\theta = \pi/2$ for acquiring the largest THz yield.[16] Three cases with different laser pulse energies are discussed in detail. For the first case, the single laser pulse energy is $W = 200$ μJ assuming 20% frequency doubling efficiency. As for the other two cases, the single laser pulse energy is increased to 25 μJ and 300 μJ respectively, keeping the relative phase and frequency doubling efficiency unchanging.

By solving Eq. (3), the time varying electron density in gas irradiated by the laser fields given above can be determined, as shown in Fig. 1. For the three cases studied, one can understand from Fig. 1 that the electron density first undergoes an increase and then saturates, and adding to the pulse energy can enlarge the available plasma electron density. However, the calculations (laser energy from 50 μJ to 500 μJ, the energy step 50 μJ) show that when the laser pulse energy is more than 300 μJ the plasma electron density does not markedly increase with pulse energy, but tends toward a stable value. Calculations indicate that at pulse energy 300 μJ, the ultimate electron density gets to about 4.9562×10^{19} cm^{-3}, meaning almost all the N_2 molecules (the main ingredient of atmospheric air) have been ionized to N_2^+, for the molecular gas initial density assumed as 5×10^{19} cm^3. From Fig. 1, one can see that the greater the pulse energy is, the faster the electron density goes up and sooner saturation is reached.

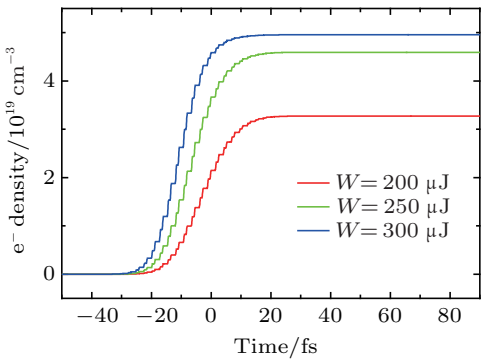


Fig. 1. (color online) Electron density of atmospheric nitrogen gas irradiated by a combined $\omega(\lambda_1 = 800$ nm) and $2\omega(\lambda_2 = 400$ nm) laser field.

Under the influence of the incident laser electric field, the ionized electrons are accelerated along the field direction and generate an electron current $J(t)$, which can be determined through solving Eq. (5), the results are shown in Fig. 2. Note that, in this calculation, transport and space charge effects are ignored. Simultaneously, the collision process of the electron–ion and electron–neutral is also not taken into account for simplicity. From Fig. 2, it is seen that adding to the laser pulse energy can greatly strengthen the electron current, owing principally to the fact that, at the larger pulse energy situation, the laser electric field is larger and more electrons are yielded. In addition, besides the oscillatory feature, a non-zero DC electron current appears after the laser pulse is gone, generating the THz emission in the far field.

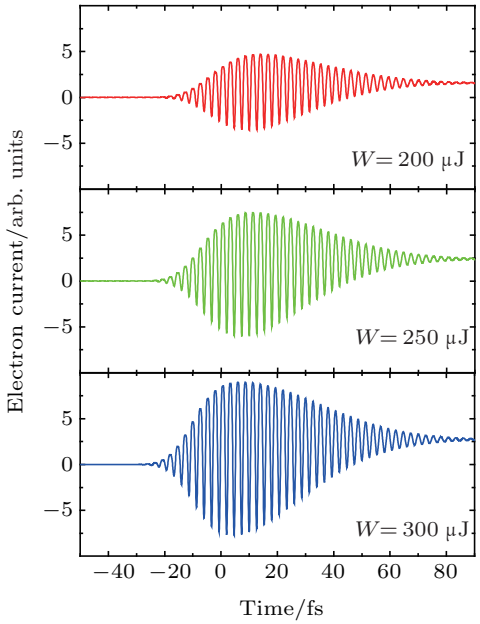


Fig. 2. (color online) Time-varying electron current for the three cases.

Computing the derivative of $J(t)$ on time t, in terms of Eq. (5), we can obtain time-varying THz emission, and the THz waveforms are demonstrated in Fig. 3 for the three specific cases. Figure 3 clearly reveals that the final THz emission can be significantly increased with the pulse energy strengthening, keeping the irradiating laser pulse width and the relative phase invariant. This may be because the ionized electron density gets larger when the laser energy is stronger, as shown in Fig. 1, which leads to a faster changing oscillating current and larger dc current as in Fig. 2, adding magnitude to the THz emission. In addition, from Fig. 3, the THz waveforms for the three cases are unchanging, which indicates that the increase of laser energy does not cause the THz spectrum to vary. Finally, one can find out that the position of the THz peak point gradually moves to the left and far away from the coordinate origin with the optical energy strengthening. This is mainly due to the fact that, when the laser energy becomes greater, the electron density goes up faster, reaching the largest value sooner, as shown in Fig. 1, which results in a decrease of the

time needed for the THz field to reach maximum, and the peak point moves to the left, far away from the coordinate origin.

By Fourier transform, the THz radiation electromagnetic spectra can be obtained, and figure 4 displays the corresponding spectra's graph for the three cases. From Fig. 4 we can see that the waveforms of the spectra do not vary very much apart from the amplitudes enlarging with the optical energy increasing, which is consistent with the analysis in the above paragraph. Furthermore, figure 4 clearly shows that the spectrum amplitudes are nearly equal to zero at greater frequency range, which is mainly ascribed to declining edge of the selected low-pass filter in the calculation.

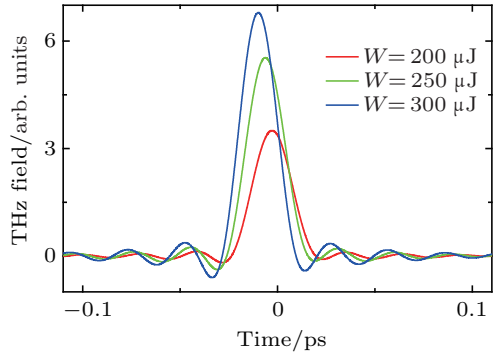


Fig. 3. (color online) THz waveforms obtained with 50-THz low-pass filtering.

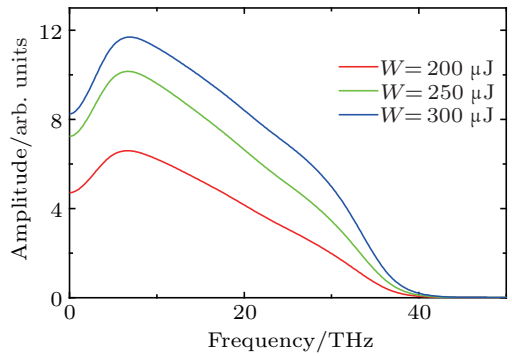


Fig. 4. (color online) The corresponding THz radiation spectra for three cases.

The dependent relationship of THz field amplitude on the laser pulse energy is computed as the optical energy is discretely changed from 50 μJ to 500 μJ, and the step is fixed at 50 μJ. Figure 5 demonstrates the calculation finding. In terms of Fig. 5, when the optical energy is beyond 100 μJ, the THz yield grows rapidly with the laser energy. However, after laser pulse energy arrives at 300 μJ, the THz output strongly tends to saturation with optical energy increasing. This saturation phenomenon can be interpreted as the strong absorption of THz emission in the gas plasma. From Fig. 5, it is very clear that THz emission is markedly enhanced with a near-linear dependency on the optical energy when the laser energy is at a moderate level, as shown with the added blue dash line.

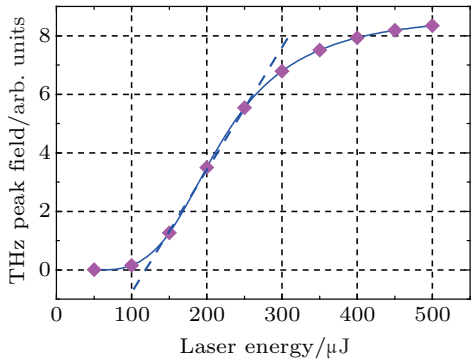


Fig. 5. (color online) THz peak field intensity versus incident laser energy. The added dashed line describes the near-linear function.

Note that in the simulations only single ionization is taken into account. Actually, our calculations show that double ionization takes place with single ionization nearly simultaneously. However, for laser energy less than 500 μJ, the double ionization rate is less than that of single ionization, and the contribution from the double ionization to THz generation can almost be ignored. A similar finding is demonstrated in Ref. [29].

4. Conclusion

In summary, we have employed the transient photocurrent model to simulate the physical process of engendering THz emission in air plasma excited by a two-color pulsed laser composed of the fundamental ω (800 nm) and the second harmonic 2ω (400 nm) pulses. The main issue in the paper is the dependence of the THz field on the incident laser energy, and three cases of optical energy, with $W = 200$ μJ, 250 μJ, and 300 μJ, were principally discussed. The electron density variation for the three cases is first calculated, and then, the electron current J is computed from $\int_{t_0}^{t} ev(t,t')\rho_e(t')\mathrm{d}t'$, and the final THz output is acquired by $\mathrm{d}J/\mathrm{d}t$. By Fourier transform, we obtained the THz radiation spectrum. Results show that increasing the incident laser pulses' energy can significantly enlarge the output THz peak field amplitude, but the THz spectrum component does not change. Finally, the dependence relationship of the THz field on the optical energy was computed through selecting ten discrete values, and the corresponding curve was plotted.

References

[1] Hamster H, Sullivan A, Gordon S, White W and Falcone R W 1993 *Phys. Rev. Lett.* **71** 2725
[2] Hamster H, Sullivan A, Gordon S and Falcone R W 1994 *Phys. Rev. E* **49** 671
[3] Cook D J and Hochstrasser R M 2000 *Opt. Lett.* **25** 1210
[4] Kress M, Löffler T, Eden S, Thomson M and Roskos H G 2004 *Opt. Lett.* **29** 1120
[5] Xu J Z, Yuan T, Mickan S and Zhang X C 2003 *Chin. Phys. Lett.* **20** 1266
[6] Myriam B, Hao Z Q, Matthieu B, Yu J, Zhang Z and Zhang J 2007 *Chin. Phys. Lett.* **24** 3466

[7] Quan D H, Liu S L, Zhang L, Yang J, Wang L, Yang G Z and Weng Y X 2003 *Chin. Phys.* **12** 986

[8] Zhang X C and Xu J Z 2009 *Introduction to THz Wave Photonics* (New York: Springer)

[9] Lei X L and Liu S Y 2001 *Chin. Phys.* **10** 840

[10] Karpowicz N and Zhang X C 2009 *Phys. Rev. Lett.* **102** 093001

[11] Dai J, Karpowicz N and Zhang X C 2009 *Phys. Rev. Lett.* **103** 023001

[12] Xie X, Dai J and Zhang X C 2006 *Phys. Rev. Lett.* **96** 075005

[13] Thomson M D, Kreß M, Löffler T and Roskos H G 2007 *Laser Photon. Rev.* **1** 349

[14] Federici J F 1991 *IEEE Trans. Plasma Sci.* **19** 549

[15] Kim K Y, Glownia J H, Taylor A J and Rodriguez G 2007 *Opt. Express* **15** 4577

[16] Kim K Y 2009 *Phys. Plasmas* **16** 056706

[17] Wang W M, Sheng Z M, Wu H C, Chen M, Li C, Zhang J and Mima K 2008 *Opt. Express* **16** 16999

[18] Wang W M, Kawata S, Sheng Z M, Li Y T and Zhang J 2011 *Phys. Plasmas* **18** 073108

[19] Wang W M, Sheng Z M, Li Y T, Chen L M, Dong Q L, Lu X, Ma J L and Zhang J 2011 *Chin. Opt. Lett.* **9** 110002

[20] Xie X, Dai J, Yamaguchi M and Zhang X C 2006 *Proc. SPIE* **6212** 62120N

[21] Rodriguez G and Dakovski G L 2010 *Opt. Express* **18** 15130

[22] Schumacher D W and Bucksbaum P H 1996 *Phys. Rev. A* **54** 4271

[23] Leemans W P, Clayton C E, Mori W B, Marsh K A, Kaw P K, Dyson A, Joshi C and Wallace J M 1992 *Phys. Rev. A* **46** 1091

[24] Corkum P B, Burnett N H and Brunel F 1989 *Phys. Rev. Lett.* **62** 1259

[25] Ammosov M V, Delone N B and Krainov V P 1986 *Sov. Phys. JETP* **64** 1191

[26] Corkum P B 1993 *Phys. Rev. Lett.* **71** 1994

[27] Rae S C and Burnett K 1992 *Phys. Rev. A* **46** 1084

[28] Delone N B and Krainov V P 1985 *Atoms in Strong Light Fields* (Berlin: Springer-Verlag)

[29] Zhang K Y, Du H W, Chen M and Sheng Z M 2012 *Acta Phys. Sin.* **61** 160701 (in Chinese)